

NUMERICAL CALCULATIONS OF RECEIVED NIGHT-TIME ATMOSPHERIC PULSE WAVEFORMS ASSUMING THE WAVEFORM RADIATED FROM A LIGHTNING STROKE AND THE IONOSPHERIC REFLECTION COEFFICIENT

KAZUO SAO

Summary—The purpose of the present paper is to give a more detailed account of reflection type atmospheric waveforms on the basis of the ray theory. The author tried to calculate individual pulse waveforms numerically assuming the waveform radiated from a lightning stroke and the ionospheric reflection coefficient.

Since numerical calculations are quite tedious to give, only several pulse waveforms are presented, and the results indicate that computed pulse shapes change, in general, from an original waveform to more distorted waveforms. The results suggested here seem to explain the properties of reflection type atmospheric waveforms.

During the reflection type night-time waveform analyses the discrepancies regarding the position of pulses of any reflection order were often found. In addition, negative pulses were sometimes adopted in waveform analyses, and the waveforms observed at a great distances had the quasi-sinusoidal or long oscillatory train type. So far as is known, little work has been done to get an idea of the properties mentioned above. The author tried to derive received pulse waveforms numerically, assuming both the waveform radiated from an origin and the ionospheric reflection coefficient. To discuss these points the method of numerical computation is described together with results obtained.

Since reflection type waveforms observed at night are interpreted by simple reflection theory, received pulse waveforms are to be obtained numerically if both ionospheric reflection coefficient and pulse waveform radiated from an origin are assumed. By differentiating the lightning discharge current during a return stroke with respect to time the radiated pulse waveform is obtained. According to the paper by Dr. Morrison the time variation of electric dipole moment is expressed as follows,

$$\frac{dM}{dt} = 2 i_0 v_0 \frac{1}{r} (e^{-\alpha t} - e^{-\beta t})(1 - e^{-\gamma t})$$

According to the above expression the radiated waveform $G(t)$ would be

$$G(t) = \alpha e^{-\alpha t} - \beta e^{-\beta t} - (\alpha + \gamma) e^{-(\alpha + \gamma)t} + (\beta + \gamma) e^{-(\beta + \gamma)t}$$

In addition, values of α , β and γ quoted in his paper are $7 \times 10^3 \text{ sec}^{-1}$, $4 \times 10^4 \text{ sec}^{-1}$ and $3 \times 10^4 \text{ sec}^{-1}$ respectively. To simplify the expression $G(t)$ if $\beta = \gamma$ and $\alpha + \beta \cong \beta$ are put, the expression $G(t)$ is rewritten in the simpler form

$$G(t) = \alpha e^{-\alpha t} + 2\beta e^{-2\beta t} - 2\beta e^{-\beta t} \tag{1}$$

Hence the frequency spectrum of (1) obtained by Fourier transformation becomes

$$S(\omega) = \int_0^{\infty} (\alpha e^{-at} + 2\beta e^{-2\beta t} - 2\beta e^{-\beta t}) e^{-j\omega t} dt = \int_{-\infty}^{+\infty} |S(\omega)| \cdot e^{j(\omega t - \theta_1 + \pi)} d\omega$$

where

$$|S(\omega)| = \sqrt{\left(\frac{2\beta^2}{\beta^2 + \omega^2} - \frac{4\beta^2}{4\beta^2 + \omega^2} - \frac{\alpha^2}{\alpha^2 + \omega^2}\right)^2 + \omega^2 \left(\frac{2\beta}{\beta^2 + \omega^2} - \frac{2\beta}{4\beta^2 + \omega^2} - \frac{\alpha}{\alpha^2 + \omega^2}\right)^2} \quad (2)$$

$$\theta_1 = \tan^{-1} \left[\frac{\frac{2\beta}{\beta^2 + \omega^2} - \frac{2\beta}{4\beta^2 + \omega^2} - \frac{\alpha}{\alpha^2 + \omega^2}}{\frac{2\beta^2}{\beta^2 + \omega^2} - \frac{4\beta^2}{4\beta^2 + \omega^2} - \frac{\alpha^2}{\alpha^2 + \omega^2}} \cdot \omega \right] \quad \theta_1 > 0 \quad (3)$$

Expressions (1), (2) and (3) are drawn in Figs. 1, 2 and 3 respectively. Introducing the following conditions,

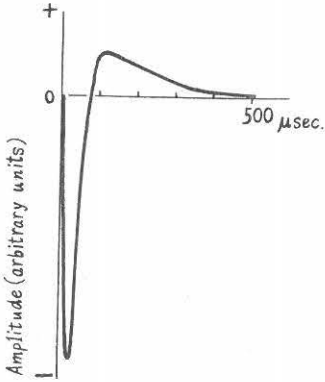


FIG. 1

$$\mu^2 \approx -j \frac{\omega_r}{\omega}$$

(μ : complex refractive index)

$$\frac{\omega_r}{\omega} \gg \sin^2 \theta \quad (\theta: \text{incident angle to the ionosphere})$$

Expression of Fresnel reflection coefficient then becomes,

$$R(\theta, \omega) = \frac{\mu^2 \cos \theta - \sqrt{\mu^2 - \sin^2 \theta}}{\mu^2 \cos \theta + \sqrt{\mu^2 - \sin^2 \theta}}$$

where

$$|R(\theta, \omega)| = \frac{\sqrt{1 + \frac{\omega_r^2}{\omega^2} \cos^4 \theta}}{1 + \frac{\omega_r}{\omega} \cos^2 \theta + \sqrt{\frac{2\omega_r}{\omega} \cdot \cos \theta}} \quad (4)$$

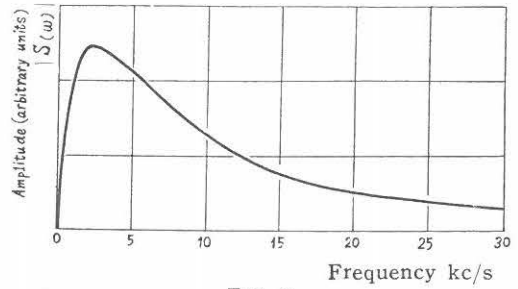


FIG. 2

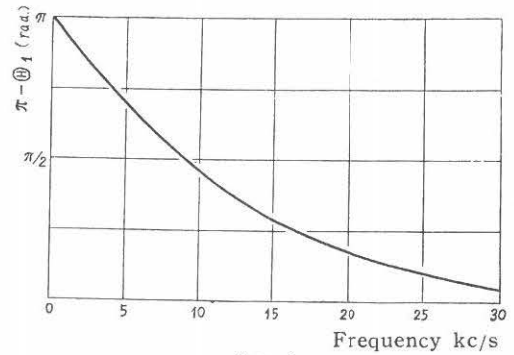


FIG. 3

$$\theta_2 = \tan^{-1} \left[\frac{\sqrt{2} \frac{\omega_r \cos \theta}{\omega}}{1 - \frac{\omega_r \cos^2 \theta}{\omega}} \right] \quad 0 > \theta_2 > -\pi \quad (5)$$

Assuming the earth is a perfect plane conductor, the received waveform reflected n times on the ionosphere is represented as follows.

$$G(t) = \int_0^{\infty} |S(\omega)| \cdot |R(\theta, \omega)|^n \cdot \cos(\omega t - \theta_1 + \pi + n\theta_2) d\omega \quad (6)$$

After all $G(t)$ can be obtained by computing (6).

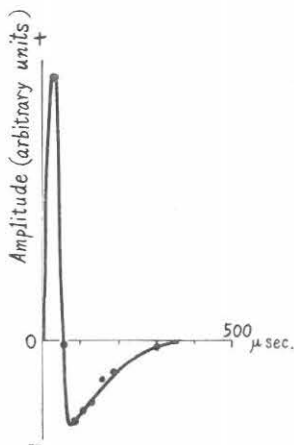
In spite of errors existing in computation by the use of a limiting processes, the author tried to derive results in the following cases. Distances from the origin, the reflection height and values of the parameter (ω_r) concerning the conductivity of the ionosphere are given in Table 1.

TABLE 1

Figure	Distance from source (km)	Reflection height (km)	Order of pulse	Parameter of ionosphere ω_r (sec ⁻¹)
Fig. 4 (A)	1,500	87	1	6×10^5
" (B)	"	"	3	"
" (C)	"	"	5	"
" (D)	"	"	7	"
Fig. 5 (A)	"	"	2	2×10^5
" (B)	"	"	5	"
Fig. 6	3,000	"	10	6×10^5

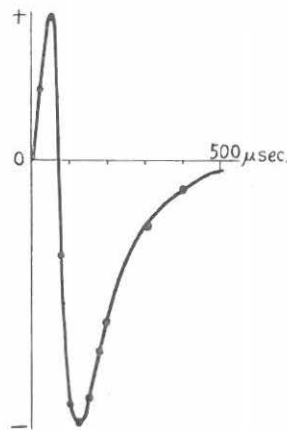
The following discussions may be derived from a study of these computed waveforms.

(1) The shapes of the individual computed pulses show marked variations from the original waveform at a source. Their predominant features are double pulses, and positive portions occur first (Fig. 4 (A), (B), (C)). One of the corresponding



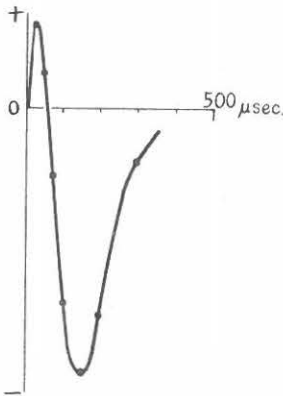
$D=1,500$ km, $h=87$ km, $\omega_r=6 \times 10^5$ sec⁻¹, $n=1$

FIG. 4 (A)



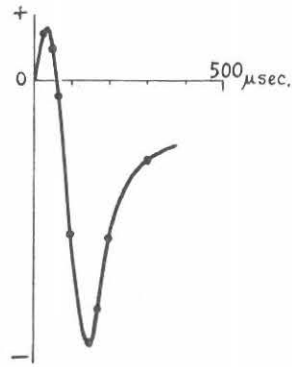
$D=1,500$ km, $h=87$ km, $\omega_r=6 \times 10^5$ sec⁻¹, $n=3$

FIG. 4 (B)



$D=1,500$ km, $h=87$ km, $\omega_r=6 \times 10^5$ sec $^{-1}$, $n=5$

FIG. 4 (C)



$D=1,500$ km, $h=87$ km, $\omega_r=6 \times 10^5$ sec $^{-1}$, $n=7$

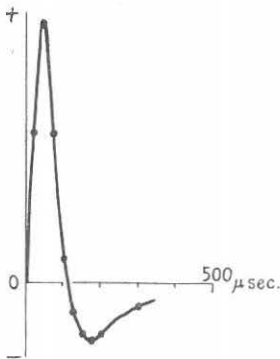
FIG. 4 (D)

observed waveforms is shown in Fig. 7. The calculated results agree very closely. Furthermore peaks are of opposite sign to that of the original waveform, and the later order pulses become predominantly negative (Fig. 4 (B), (C), (D)).

That this is so has been confirmed experimentally waveform analyses. According to Dr. Pierce successive negative peaks are adopted, for their peaks are generally more pronounced than the positive maxima.

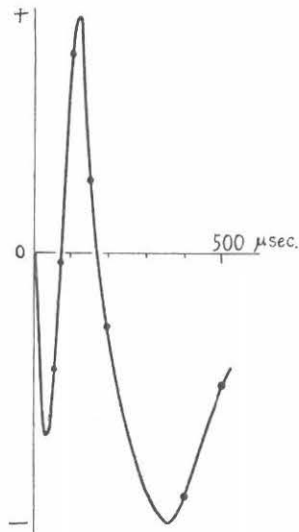
(2) When the value of ω_r decreases, the calculated pulse waveforms (Figs. 5 (A), (B)) become more complicated than the ones described above (Fig. 6).

If such individual pulses as shown in Fig. 7 are superimposed successively in



$D=1,500$ km, $h=87$ km, $\omega_r=2 \times 10^5$ sec $^{-1}$, $n=2$

FIG. 5 (A)

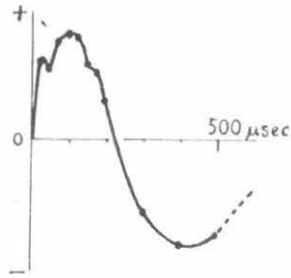


$D=1,500$ km, $h=87$ km, $\omega_r=2 \times 10^5$ sec $^{-1}$, $n=5$

FIG. 5 (B)

order to get a night-time reflection type complete waveform, more complex waveform will be expected, frequently overlapping the preceding and following pulses.

(3) The calculated late-order pulse waveform received at a great distance has a rounded character shown in Fig. 6. The change from a peaked to a smooth



$D=3,000$ km, $h=87$ km, $\omega_r=6 \times 10^5 \text{sec}^{-1}$, $n=10$

FIG. 6

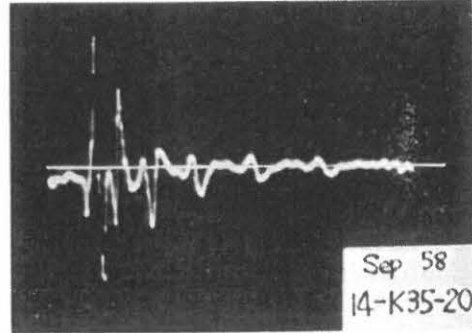


FIG. 7

waveform with increasing order and with increasing distance is consistent with the individual pulse of quasi-sinusoidal or long oscillatory train type atmospheric waveforms.

(4) As is shown in Fig. 6, negative peaks reach their maxima about $150 \mu\text{s}$ later than the beginning of the waveforms.

Hence, provided that the ground pulse or first order pulse reach their maxima soon after their beginning, the positions of their peaks are removed from those of late-order peaks. This fact is in accordance with the investigation, by Dr. Hepburn and Dr. Pierce. According to their papers it was often desirable to adopt a peak of comparatively late order as the reference peak, and extrapolation back to the start of the waveform yielded the surprising result that there was a frequent substantial portion of the atmospheric, of up to half a millisecond duration, occurring before the disturbance corresponding to the ground wave of the reflection theory solution. The numerical results have an interesting bearing on the nature of observed waveforms.

Several points concerning the night-time reflection type atmospheric waveforms seem to have come to light during the course of this work.

Finally, the author wishes to express his gratitude to Director Kimpara of our Institute for his constant encouragement and advice in his study. The assistance of Miss Maeda during the computation and in the preparation of this paper is deeply acknowledged.